Environment, Development and Sustainability (2021) 23:9397–9417
https://doi.org/10.1007/s10668-020-01031-2

Time–frequency co-movement between COVID-19, crude oil prices, and atmospheric CO_2 emissions: Fresh global insights from partial and multiple coherence approach

Yasir Habib[1] · Enjun Xia[1] · Zeeshan Fareed[2] · Shujahat Haider Hashmi[3]

Received: 9 August 2020 / Accepted: 30 September 2020 / Published online: 11 October 2020

Abstract

This paper endeavors to analyze and provide fresh global insights from the asymmetric nexus between the recent outbreak of COVID-19, crude oil prices, and atmospheric CO_2 emissions. The analysis employs a unique Morlet's wavelet method. More precisely, this paper implements comprehensive wavelet coherence analysis tools, including continuous wavelet coherence, partial wavelet coherence, and multiple wavelet coherence to the daily dataset spanning from December 31, 2019 to May 31, 2020. From the frequency perspective, this paper finds significant wavelet coherence and vigorous lead and lag connections. This analysis ascertains significant movement in variables over frequency and time domain. These results demonstrate strong but varying connotations between studied variables. The results also indicate that COVID-19 impacts crude oil prices and the most contributor to the reduction in CO_2 emissions during the pandemic period. This study offers practical and policy implications and endorsements for individuals, environmental experts, and investors.

Graphic abstract

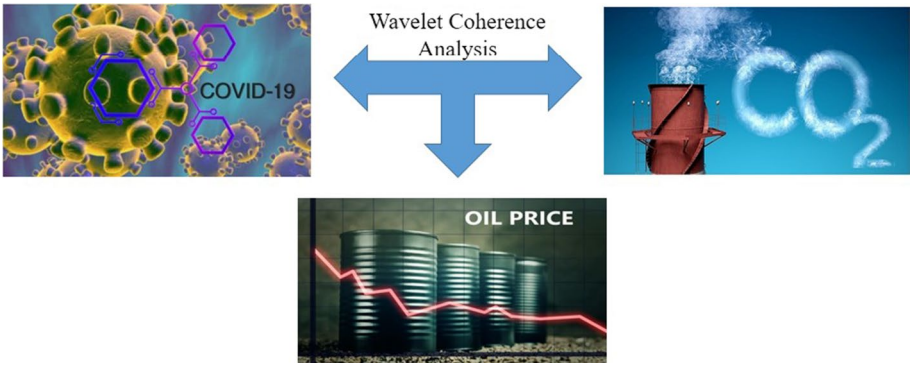

Keywords COVID-19 · Crude oil prices · Atmospheric CO_2 emissions · Partial and multiple wavelet coherence · Global

Extended author information available on the last page of the article

1 Introduction

Since late December 2019, a new contagious disease in the family of coronavirus was spotted in Wuhan City, China, later named *the Coronavirus Disease 19* (COVID-19), a causative agent of pneumonia (Lu et al. 2020; Xu et al. 2020). It has impeded economic development and strained healthcare delivery networks worldwide. COVID-19 is a new type of coronavirus and is caused by *severe acute respiratory syndrome coronavirus 2* (SARS-CoV-2) (Di Gennaro et al. 2020; Dong et al. 2020; Huang et al. 2020; Sohrabi et al. 2020; Zhou et al. 2020). SARS-CoV-2 has a higher contagious capacity than middle east coronavirus respiratory syndrome (MERS-CoV) and severe acute respiratory syndrome (SARS), a zoonotic beta (pathogenic) viral respiratory disease triggered by severe acute respiratory syndrome coronavirus (SARS-CoV-1or SARS-CoV-2). In general, most SARS-CoV-2 infected patients have common mild symptoms, including dry cough, fever or chills, fatigue, diarrhea, myalgia, sore throat, and conjunctivitis (Huang et al. 2020; Sohrabi et al. 2020). Nevertheless, some patients could have severe and even deadly complications such as multiple organ failure, septic shock, shortness of breath, pulmonary edema, severe pneumonia, and acute respiratory distress syndrome (ARDS) (Chen et al. 2020).

SARS-CoV-2 is transmitted primarily through close and direct interaction between humans, respiratory and pulmonary droplets, fomites, and infected surfaces and substances. It is analogous to the transmission of other respiratory tract viruses or infections such as influenza or human Boca virus (coronavirus) (Lai et al. 2020; WHO 2020a). World Health Organization (WHO) confirmed the human transmission of COVID-19 by airborne droplets to humans in January 2020 (WHO 2020a, b). On December 31, 2019, authorities reported a spike of confirmed COVID-19 cases in Wuhan City, which proliferated not only in the neighboring counties but also spilled throughout the country and, after a month, this new coronavirus outbreak turned into an epidemic from just beyond the community (Chan et al. 2020; Dutheil et al. 2020). In the last week of January 2020, Wuhan City was quarantined, and within a few days, the Hubei Province follows. In an effort, the Chinese government imposed increasingly stringent measures to isolate the symptomatic cases, slow down infection spread, avoid person-to-person transmission, and ease the burden on the healthcare system (Gautam and Hens 2020a; Le Quéré et al. 2020; Wilder-Smith and Freedman 2020). As of January 30, 2020, the WHO set a global public health emergency (Gautam and Hens 2020b; WHO 2020c). In mid-February, the global outbreak starts in South Korea, Iran, Japan, Europe (primarily Italy, France, and Spain), and the USA. Eventually, the emergence of the COVID-19 transforms into a pandemic, and before the end of March, a large proportion of the world's population was under some sort of locked down (Cucinotta and Vanelli 2020; Tosepu et al. 2020). From September 27, 2020, the aggregate number of COVID-19 infected cases outstripped 32.92 million worldwide, and the death toll to 9,95,145 (ECDC 2020). Figure 1 shows the global daily new infected and confirmed cases of COVID-19 from December 31, 2019, to May 31, 2020.

When countries entered into lockdown, global manufacturing and economic activities were shutdowns. Transport, among many other sectors, is the most affected business by the lockdown. By the end of March 2020, worldwide road transportation mobility was almost 50% below the average of the Q1 2019 level. Nonetheless, as lockdowns extent, global air travel plummeted a staggering 60% by the end of Q1 2020 (OAG 2020). Worldwide demand for crude oil and prices declined dramatically by 5% and 6.6%, respectively, in Q1 2020, due to curtailment in aviation and road mobility, accounting for approximately 60% of global oil demand (IEA 2020). Figure 2 shows the daily crude oil price USD per

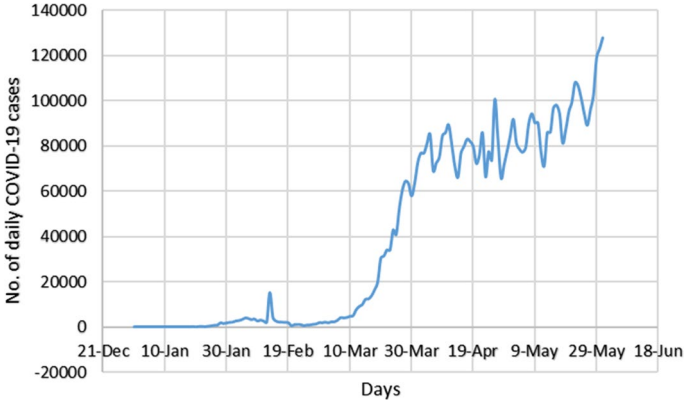

Fig. 1 Daily new infected and confirmed cases of COVID-19

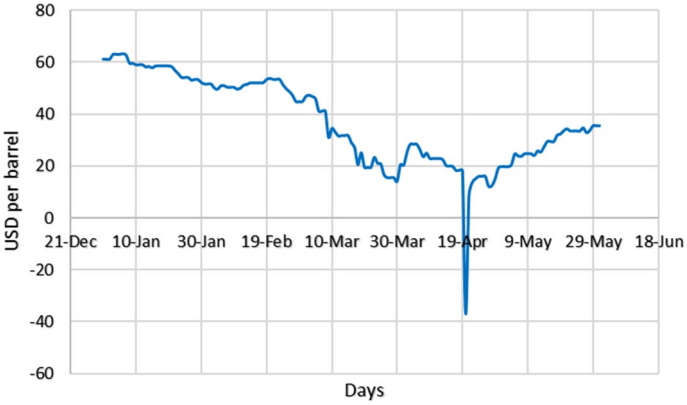

Fig. 2 Daily crude oil price USD per barrel

barrel from December 31, 2019 to May 31, 2020. Also, not only the transportation sector but also the other industrial and production units are severely affected by the pandemic. COVID-19 has significant negative impacts on human health and the global economy but also contributes to decreased CO_2 emissions as a result of less oil demand, population confinement, and less industrial activities (Dutheil et al. 2020; Le Quéré et al. 2020). The epidemic of COVID-19 has been attributed to the dramatic changes in air quality. Therefore, lockdown, due to this attributed epidemic spread, reduced economic, and transportation activities, resulted in lower energy consumption and lower oil demand. Such shifts in transport and industrial operations and oil demand have a substantial effect on the quality of the environment.

Most of the global regions reported a drastic drop in air pollution as an expected side effect of this unparalleled lockdown. For instance, the air pollution level is decreased in the cities of the UK up to 60% compared to the same period in 2019 (BBC 2020). In China, CERA (Centre for Research on Energy and Clean, Finland) and NASA (National Aeronautics and Space Administration) announced that COVID-19 combating initiatives, such as traffic restrictions and closure of industrial units and power plants, resulted in a 25–30%

reduction in CO_2 emissions (Carbon Brief 2020; NASA Earth Observatory 2020a). According to the report, the air pollution level over New York (USA) and New Delhi (India) was 30% and 60% lower in March, respectively, as compared to the same month in 2019 (NASA 2020; NASA Earth Observatory 2020b). Likewise, a satellite image from the European space agency (ESA) revealed a substantial decrease in emissions in northern Italy from January 1 to March 11, 2020, correlating with lockdown to counter coronavirus (ESA 2020). In Asia and Europe, European Space Agency (Sentinel-5P satellite) measurements show that air pollution levels over cities and industrial areas were lower by as much as 40% during the same period in 2019 at the end of January and early February 2020 (The Conversation, April 15, 2020). On March 16, 2020, the Department of Environment and Natural Resources reported that since the effectuation of the Luzon enhanced community quarantine, Metro Manila's emissions have been substantially reduced as a result of lessened use of crushing and grinding machines as well as low road dust exposure (CNN 2020).

To study PM2.5 concentrations changes under CO_2 emission reduction scenarios, Wang et al. (2020) empirically found that anthropogenic emissions decrease due to the transportation and industry suspension, leading to PM2.5 concentration decreases. Mitra et al. (2020) aligned atmospheric CO_2 emissions levels, directing on Indian city, Kolkata, between April 2019 (pre-COVID-19 phase) and April 2020 (lockdown phase). The authors observed a substantial difference in atmospheric CO_2 emissions levels between periods, but no shift between spots, using data from 12 various locations. Thus, as the critical determinants of CO_2 emissions are factories and transports, (Mate et al. 2020; Mitra et al. 2020) inferred this finding as a pronounced lockdown effect attributable to COVID-19. Recent studies (Aydın et al. 2020; Huang et al. 2020) investigated the patterns of primary and secondary air pollution emissions in Turkey and China during the COVID-19 lockdown and highlighted the relation between these two pollutants. Both authors have an estimate of the decline in provincial emissions of primary and secondary air contaminants. Both studies illustrate an important point: while the COVID-19 lockdown created a significant reduction in primary and secondary air pollution emissions, these are temporary improvements and will not prevent severe degradation of air pollution emissions in China and India in the long run. So, there is a vast space for furtherance.

Anjum (2020) built a comprehensive appraisal framework on COVID-19 restrictions and changes in air quality and also indicated that the temporary countrywide lockdowns first resulted in apparent substantial reductions in air pollution. Urrutia-Pereira et al. (2020) empirically found that significant declines in anthropogenic emissions owing to factories, construction sites, gas stations transport, and industry suspensions have led to a reduction in atmospheric particulate matter in the major cities of China.

The literature review highlights that a significant chunk of prior empirical studies has mainly focused on the role of the pandemic is affecting the environment in either a single country-setting, city-level scenario or by utilizing estimated CO_2 emissions. The empirical studies on individual countries or cities provide useful insights into specific changes in environmental quality. Still, they fail to deliver the pervasive and widespread impact of COVID-19 on the environment. In addition, estimated figures of carbon emissions from recent data may not truly reflect the atmospheric effect of the pandemic, which suddenly ceased all the socioeconomic activities in the world. Therefore, projections based on previous trends could be misleading and underestimated.

Moreover, the spread of pandemic (COVID-19) affected carbon emissions via the channel of energy consumption and demand, which have been overlooked in prior studies. The sudden outbreak of COVID-19 caused a significant decline in energy demand, especially

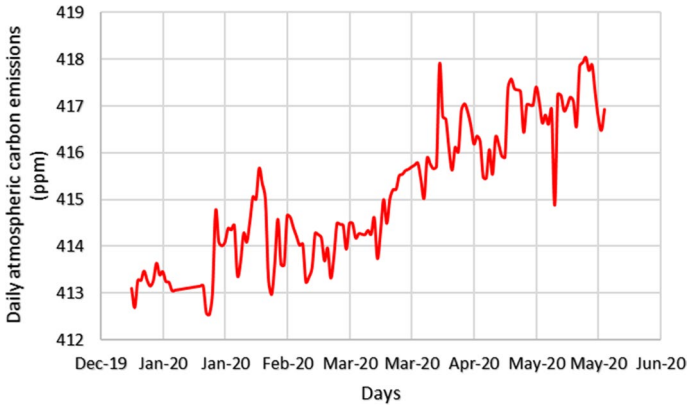

Fig. 3 Daily atmospheric CO_2 emissions (ppm)

fossil fuel consumption, significantly affecting the oil prices in the world. The worldwide transportation system has come to a standstill because the pandemic caused a sharp decline in the mobility of goods and people and adversely affected the economies. The lower level of economic activities has, thus, decreased energy demand and oil prices, affecting the overall environmental sustainability in the world. Another major issue with the prior studies is they assume the monotonic or linear relationship between COVID-19 and environmental pollution. Due to the complex atmospheric chemistry, there are still open questions during the epidemic concerning the composition of air pollution and spatiotemporal patterns. However, in reality, the global pandemic may have affected the environment asymmetrically over the different phases of its outbreak, which requires further investigation. Therefore, the objective of the current study is to investigate the asymmetric co-movement linkage between COVID-19, oil prices, and atmosphere carbon emissions in a global setting by applying an advanced and innovative wavelet approach. Figure 3 shows the daily atmospheric CO_2 emissions (ppm) (hereafter CO_2 emissions) from December 31, 2019 to May 31, 2020.

Our empirical work contributes to previous literature in the following manner. First, our unique study is innovative and pioneer in the sense because it studies the simultaneous co-movements between COVID-19, oil prices, and atmospheric CO_2 emissions. The interesting thing about reviewing the literature for this study is that most of the studies are focused on mean prejudices from lockdown (February–May 2020) compared to the same period of 2019, subject to emission anomalies, weather conditions, and world economy. The world economy faces two acute shocks: the outbreak of the deadly COVID-19 contagion and the unprecedented crude oil price slump. The assortment of these two issues will likely cause a long-term economic decline into recession and short-term reduction in CO_2 emissions and environmental healing. These are the motivating concerns for this study. Based on these arguments, it will be the first endeavor to investigate the cohesiveness and the lead–lag linkage between the COVID-19, CO_2 emissions, and crude oil prices across a time–frequency based approach. The pandemic mainly affects the environment through worldwide energy demand (primarily fossil fuel sources), as reflected in world oil prices. Therefore, our research fills the previous gap by including this oil energy demand channel. Second, our study applies the innovative and robust method to investigate the asymmetric co-movement interactions between considered variables. Therefore, we turn to wavelet

coherence analysis to accomplish this task. In particular, we adopt the continuous wavelet analysis tools, mainly wavelet transform coherence, partial wavelet coherence, and multiple wavelet coherence tests on recent daily global data.

On the methodological frontier, by using wavelet coherence analysis, a method that funnels the data from time and frequency, we distinguish our study from the substance of the empirical research. To probe the nonlinear co-movement and the lead–lag connections among COVID-19, CO_2 emissions, and crude oil prices in the time–frequency spheres and data sample size, the conventional times series techniques, specifically, Granger causality analysis, the vector autoregressive models (VARs), generalized autoregressive conditional heteroscedastic processes (GARCH), are not suitable for the current study. These time series techniques only seize the information from the time domain but overlook the information from the frequency domain. Especially when using the wavelet method, there is plenty of space for more contributions. At least three main distinct facets stimulate the wavelet coherence use. First, with the wavelet coherence approach, we assess the association between these selected variables within the time and frequency bands. On this basis, we assume that the association between COVID-19, CO_2 emissions, and the prices of crude oil will vary in a time–frequency domain. A vital feature of wavelets is their ability to reveal underlying processes characterizing these time series with evolving cycle patterns, tendencies, lead–lag interfaces, and non-stationary ones. Second, when the interactive lead–lag connection between the used time series is nonlinear, wavelet methods are appropriate. Here, we conjecture the nonlinear effect that can also be traced across short- and long-run frontiers to heterogeneous prospects. Third, the timeliness of data is a critical issue. For a better understanding of temporal reduction in CO_2 emissions during the COVID-19 pandemic, this study used real-time CO_2 emissions data to capture the real picture for a short period. In the global epidemic, real-time atmospheric CO_2 emissions are a better measure of environmental quality than estimated and human-based CO_2 emissions because all human-based social and economic activities are shut down due to lockdown and other confined measures of this pandemic. Lastly, apart from theoretical and literature contributions, this analysis not only provides a theoretical framework for future studies to determine the environmental and economic effects of COVID-19 but also enriched the literature by extending the conceptual framework of the economy–pollution relationship from an emergency–environment–economy perspective. This study fills this void.

The remainder of paper is organized as follows. Section 2 explains the data and methodology employed in this study. Section 3 presents the empirical results, while Sect. 4 concludes the study and offers policy recommendations.

2 Data and methodology

2.1 Data

In this study, the COVID-19 outbreak is signified by the "number of global daily new infected and confirmed cases" of the COVID-19. The numbers of COVID-19 cases are obtained from the European Centre for Disease Prevention and Control.[1] The data on global daily real-time atmospheric CO_2 emissions [measured as parts per million (ppm)]

[1] The data of COVID-19 downloaded from the website https://www.ecdc.europa.eu/en/covid-19-pandemic.

are gathered from the ESRL Global Monitoring Laboratory[2]. The data of daily crude oil prices (measured as WTI standard) are compiled from DataStream. For this study, all dataset values are included on daily basis from December 31, 2019 to May 31, 2020.

2.2 Methodology

The wavelet transform provides decay of localized frequencies, including specifics on frequency components. Consequently, if the object being studied is non-uniform and locally stationary, wavelets have substantial benefits over simple Fourier analysis (Gençay et al. 2001; Percival and Walden 2000; Ramsey 2002). The wavelet approach has distinctive features as compared to other traditional time series techniques. We can evaluate stationary to non-stationary and non-normally distributed data efficiently by allowing much more flexibility in all frequencies embedded in time series analysis. The main attribute of this approach is its ability to categorize the divergent (positive and negative) forms of associations simultaneously. It is very instrumental in catching the nonlinear relationship and also assessing the association's intensity and direction while specifying the relationship between short-, medium-, and long-term frequency modules at the same time. The wavelet approach can define the extent of the local correlation (lead–lag relationship) between two-time series in a (specific) time–frequency domains and also seize the connections of nonlinearity between numerous series of data (Benhmad 2012; Vacha and Barunik 2012). Besides, in the essence of Granger causality testing, this visual staging of the wavelet coherence transform [squared coefficient $R^2(m,n)$] can confirm the existence of causal relationships between the two-time series (Goodell and Goutte 2020). However, like other advanced asymmetric time-series models, this approach is constrained by selecting typically two or three variables at most for investigating co-movement nexus between considered variables for better comprehension and focused spatial analysis. This technique can provide us better results and a clear understanding of the phenomenon under consideration due to the benefits mentioned above. That is why it is widely used in signal processing modeling and atmospheric and oceanic technology.

This paper employs the comprehensive wavelet coherence analysis tools, including wavelet transform coherence as well as continuous, partial and multiple wavelet coherence, to enclose the association and co-movement between global daily new infected and confirmed cases of COVID-19, global daily CO_2 emissions, and daily crude oil prices across time scales. Before introducing the wavelet transform coherence, we need to define the continuous wavelet transformation first.

2.2.1 The continuous wavelet transform (CWT)

Through the optimization of a specific wavelet, the transformation of continuous wavelet beside the time sequences $x(t) \in L^2(\mathbb{R})$, i.e., is achieved.

$$W_x(m,n) = \int_{-\infty}^{\infty} x(t) \frac{1}{\sqrt{n}} \overline{\psi\left(\frac{t-m}{n}\right)} \mathrm{d}t, \tag{1}$$

[2] The data of atmospheric CO_2 emissions obtained from the website https://www.esrl.noaa.gov/gmd/ccgg/trends/gl_data.html.

where m is the scale parameter and represents the specific wavelet extension and n denotes to the location that can capture the time information. The propensity to decompose and, after that, reconfigure a time series $x(t) \in L^2(\mathbb{R})$. with perfection is an essential feature of the continuous wavelet transform.

$$x(t) = \frac{1}{C_\psi} \int_0^\infty \left[\int_{-\infty}^{\infty} W_x(m,n)\psi_{m,n}(t)\mathrm{d}u \right] \frac{\mathrm{d}n}{n^2}, n > 0. \tag{2}$$

Also, the continuous wavelet transformation retains the impetus of the time series studied.

$$\| x \|^2 = \frac{1}{C_\psi} \int_0^\infty \left[\int_{-\infty}^{\infty} |W_x(m,n)|^2 \mathrm{d}m \right] \frac{\mathrm{d}n}{n^2}. \tag{3}$$

This property is used in this current paper to elucidate the wavelet coherence that quantifies the dimension of the natural inference between the structure of two-time series.

2.2.2 The wavelet transform coherence (WTC)

To investigate the interface between two series, a bivariate structure called wavelet coherence must be implemented. Despite time series, the wavelet coherence approach is commonly used. Primarily, for a better understanding of the wavelet coherence, this study needs to describe cross-wavelet transformation first and then cross-wavelet power between two-time series. Torrence and Compo (1998) have defined the two-time series paradigm for cross-wavelet transform of $W_x(m, n)$ by *x(t)* and $W_y(m, n)$ by *y(t)* in the following ways:

$$W_{\mathrm{xy}}(m,n) = W_x(m,n)W_y^*(m,n), \tag{4}$$

where m denotes location index, and n epitomizes the degree. However, the symbol of * signifies composite conjugate. With the absolute squared value of the cross-wavelet transform $|W_{xy}(m, n)|$, the cross-wavelet spectrum can easily be calculated. The cross-wavelet power spectrum is a cumulus of enclosed variance that divides the regions of intensive power density similar to those time sequences in the time–frequency space. The wavelet coherence differentiates those regions in a specific time–frequency domain where unanticipated and prominent anomalies occur in the co-movement pattern of the time-series. Adopting the Torrence and Webster (1999) framework to formulate the mathematical equation for wavelet transforms coherence is infra;

$$R^2(m,n) = \frac{|N\left(N^{-1}\left|W_{\mathrm{xy}}(m,n)\right|^2\right)}{N\left(N^{-1}\left|W_x(m,n)\right|^2\right)N\left(N^{-1}\left|W_y(m,n)\right|^2\right)}. \tag{5}$$

R is viewed as a smoothing operator, with the squared coefficient of wavelet transform coherence (WTC) range from:

$$0 \le R^2(m,n) \le 1, \tag{6}$$

if the value proximity to "0" indicating weak or no coherence; conversely, if the value proximity to "1" denoting the existence of robust coherence. In the first step, "Morlet wavelet" is used to transform the data for "Continuous Wavelet Transform" and then applied wavelet transform coherence to ascertain the co-movements of two variables. In this study, the wavelet transform coherence is examined through the method of Monte Carlo simulation. The comprehensive wavelet approach has been adopted from prior studies (Aloui et al. 2018; Hkiri et al. 2018; Ng and Chan 2012).

2.2.3 The partial wavelet coherence (PWC)

This method analyzes the co-movements of two different variables, while the unique impact of a third variable is eliminated. The mathematical portrayal of partial and wavelet transform coherence with various combinations of variables transcribed in the following terms:

$$R(x_1, x_2) = \frac{S\left[W(x_1, x_2)\right]}{\sqrt{S\left[W(x_1)\right] S\left[W(x_2)\right]}}; \tag{7}$$

$$R^2(x_1, x_2) = R(x_1, x_2) \cdot R(x_1, x_2)^*; \tag{8}$$

$$R(x_1, x_3) = \frac{S\left[W(x_1, x_3)\right]}{\sqrt{S\left[W(x_1)\right] S\left[W(x_3)\right]}}; \tag{9}$$

$$R^2(x_1, x_3) = R(x_1, x_3) \cdot R(x_1, x_3)^*; \tag{10}$$

$$R(x_2, x_3) = \frac{S\left[W(x_2, x_3)\right]}{\sqrt{S\left[W(x_2)\right] S\left[W(x_3)\right]}}; \tag{11}$$

$$R^2(x_2, x_3) = R(x_2, x_3) \cdot R(x_2, x_3)^*; \tag{12}$$

$$\mathrm{RP}^2(x_3, x_1, x_2) = \frac{\left|R(x_3, x_1) - R(x_3, x_2) \cdot R(x_3, x_1)^*\right|^2}{\left[1 - R(x_3, x_2)\right]^2 \left[1 - R(x_2, x_1)\right]^2}, \tag{13}$$

where "R" signifies the coherence between two variables, though "x_1", "x_2", and "x_3" depict the concern variables. The above-mentioned mathematical equations (7), (8), (9), (10), (11), and (12) symbolize WTC between all three possible synopses of variables "x_1", "x_2", and "x_3". The mathematical formulation of PWC in Eq. (13) finds the wavelet transform coherence between two different time series "x_1" and "x_3", and then canceling the specific effect of an added variable "x_2" for this association (Mihanović et al. 2009). In this study, the method of Monte Carlo simulation used to compute the significance level in wavelet coherence analysis (Grinsted et al. 2004).

Table 1 Summary of descriptive statistics and correlation matrix

Variable	COVID-19	CO_2	OLP
Obs	153	153	153
Mean	39,400.82	415.059	37.025
SD	40,835.1	1.511	16.873
Min	0	412.54	−36.98
Max	128,000	418.04	63.27
Jarque–Bera	18.58	10.34	7.382
P value	0.000	0.006	0.025
Correlation matrix			
COVID-19	1		
CO_2	0.902*	1	
	0.000		
OLP	−0.737*	−0.713*	1
	0.000	0.000	

* shows significance level at the 0.01

2.2.4 The multiple wavelet coherence (MWC)

The primary method to comprehend the MWC is to equate it with the multiple correlation coefficient. A co-movement is probed between one x_3 predicted variable, and the integration of two x_1 and x_2, other predictor variables, are studied. The MWC framework can be structured in the following lieu:

$$\mathrm{RM}^2(x_3, x_2, x_1) = \frac{R^2(x_3, x_1) + R^2(x_3, x_2) - 2\mathrm{Re}\left[R(x_3, x_1) \cdot R(x_3, x_2)^* \cdot R(x_2, x_1)^*\right]}{1 - R^2(x_2, x_1)}, \tag{14}$$

where "RM^2" provides the proportion of wavelet power and dependence of variable "x_3", which is explained by the linear combination of the other two "x_1" and "x_2", desired variables, respectively (Mihanović et al. 2009; Ng and Chan 2012).

3 Results and discussion

This paper strives to probe the causality of time–frequency amid COVID-19, CO_2 emissions, and crude oil prices. From prior pragmatic studies, descriptive statistics are used to evaluate and grasp the univariate characteristics of the understudy variables. Table 1 shows the descriptive statistics; we observed that the average of daily COVID-19 new confirmed and infected cases is 39,400.82, varying from a minimal number of "0" to a maximal number of 128,000 during our observation period. The mean value of COVID-19 exhibits the maximum level of volatility as compared to other variables due to the maximum standard deviation. The average daily CO_2 emissions are 415.059 parts per million (ppm), varying from a minimum of 412.54 parts per million to a maximum of 418.04 parts per million. The average daily price for crude oil is 37.025 USD per barrel, with substantial fluctuation between the minimum daily oil crude price − 36.98 USD per barrel and maximum daily crude oil price 63.27 USD per barrel. The Jarque–Bera test discloses the non-normal essence of all the studied variables. Aside from descriptive statistics, the correlation

coefficient (0.902) is positive and significant for COVID-19 and CO_2 emissions; negative (− 0.737) for COVID-19 and crude oil prices; and (− 0.713) for CO_2 emissions and crude oil prices are negative and significant alike.

Of these three variables, the upshots of continuous wavelet transform are evinced in Fig. 4. The colored graph depicts an analysis of the variables by time–frequency (scale). The *x*-axis sketched the time scale, and the *y*-axis walled the period or frequency. Within the figure, the cone of influence is mapped, and it depicts that the transform coefficients within the region are robust. The wavelet transform scale is shown on the right side. The predominant areas of interest are the red regions encircled by the orange-yellow outline. Figure 4a reveals the data movement in a three-dimensional graph, that is, time, frequency, and color band. Figure 4a indicates the continuous wavelet transform of new confirmed and infected cases of COVID-19. Red color means high power or significant variation, but the blue color illustrates low power or no considerable variation. Two small but strewn islands reveal substantial variance in the frequency scales of 0–4 between 3rd, 7th, and 8th week of the observations, respectively. An even more small shady red-colored loops are also existent on the top left corner during the first and second weeks of inferences in the frequency realm 0–4 and 4–8 and show the soaring pattern for the whole graph exceeding cone of influence (COI).

Figure 4b corresponds to the continuous wavelet transform of global daily CO_2 emissions. Two small dark red-colored oval shapes with black outlines are apparent 4–8, and 8–16 frequency domains during 4th and 5–6th, 7th, and 8th weeks of the observation period, respectively. By observing Fig. 4b, three long and one medium oval-shapes are visible at frequency regions 0–4 and 4–8 during 14th, 20th, and 6th weeks of the inference period, respectively. These small and long encircled shapes show significant and high energy patterns in CO_2 emissions during the given period.

Figure 4c discloses the continuous wavelet transform of crude oil prices. A dark red-colored "I" long shape with black outlines unveils substantial variability at the frequency spectrum 0–4, 4–8, and 8–16 during the 16–17th and 18th week of the inference cycle, respectively.

Figure 5a portrays the wavelet transform coherence between new confirmed and infected cases of COVID-19 and CO_2 emissions. Several dark red colored oval and island shapes can be found incoherent across the figure within the thick black lining. By observing Fig. 5a, the direction of small arrow clusters observed indicates the relationship trajectory between COVID-19 and CO_2 emissions. However, the right side multi-colored bar conveys the intensity of this correlation. The arrow's direction toward the right (left) displays a positive (negative) and in-phase (out-phase) connotation between these two-time series. The arrow's movements inside the contour constitute a significant co-movement. A dark red red-colored significant oval shape can be ascertained at a frequency region of 4–8 during the 6th and 7th week of the inference period, respectively. The direction of arrows from left and upward inside the oval shape implies anti-phase coherence directing from CO_2 emissions to COVID-19. This coherence inferred a negative link between COVID-19 and CO_2 emissions and is characterized by an anti-cyclical effect during this specific time–frequency realm. Two significantly large red areas are identified with the black lining. One island shape is found in the frequency realm 4–8 during the 15th, 16th, and 17th week, but the other one lies on the top left corner in the frequency range from 0 to 4 and 4 to 8 during the 2nd week of the period. The direction of arrows from right and upward inside these islands implies in-phase coherence directing from CO_2 emissions to COVID-19. This coherence implies a positive link between COVID-19 and CO_2 emissions during our observation period. On the bottom, a large red area is prominent in a circle pointing small

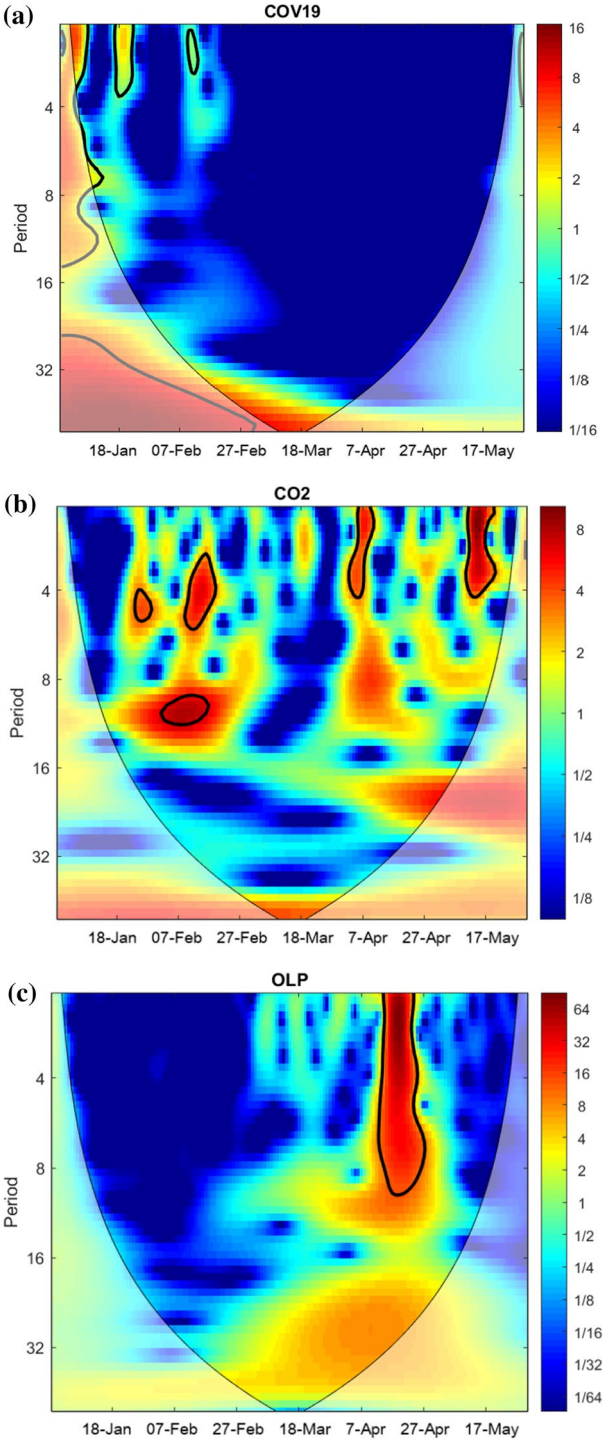

Fig. 4 Continuous wavelet transform of COVID-19, CO_2 emissions, crude oil prices

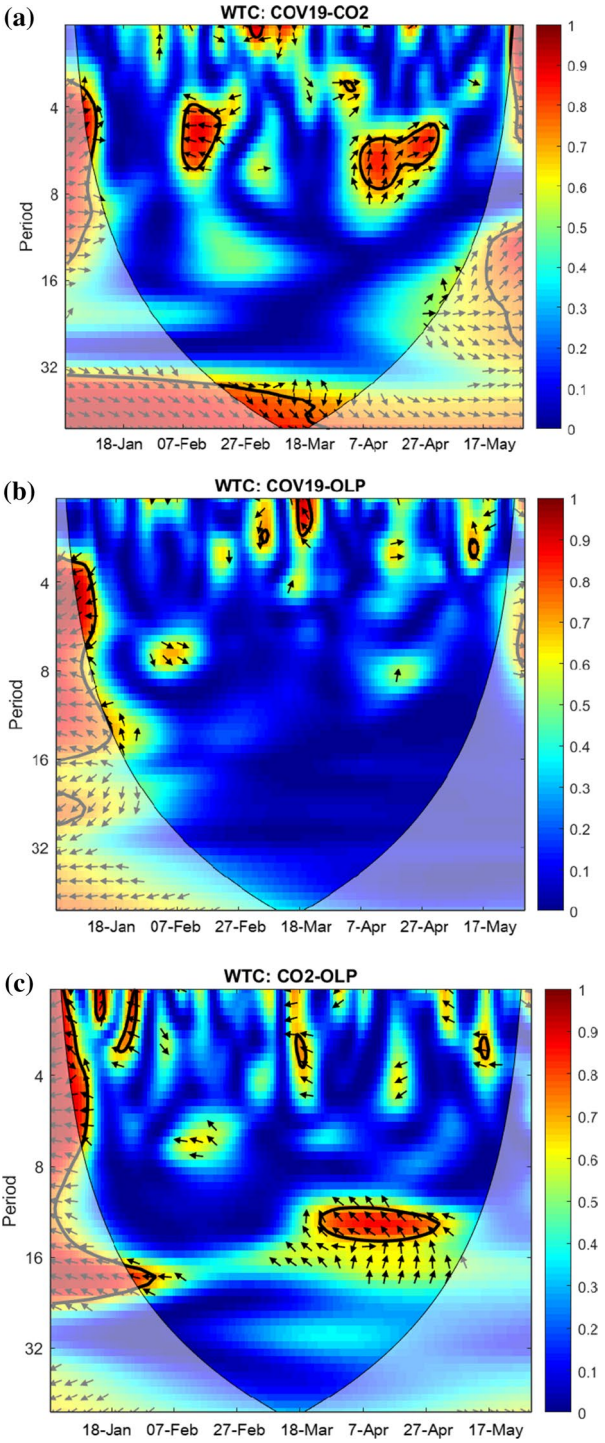

Fig. 5 Wavelet coherence transform of COVID-19, CO_2 emissions, and crude oil prices

arrows toward the right and downward in a frequency band of 32 onward during the 8th to 12th week of the observation. In the long run, in-phase coherence is observed between COVID-19 and CO_2 emissions. We note that CO_2 emissions are leading, and COVID-19 is lagging. The dark red color of shapes within the thick black line is identical with the ranging of coherence value on the right side multi-colored bar from 0.90 to 1; it reflects a robust COVID-19 effect on CO_2 emissions. From top to bottom, we can identify the black cone called "cone of influence," and denotes the level of significance and the essential edge effects along the frontiers on both sides.

Figure 5b portrays the wavelet transform coherence between COVID-19 new confirmed and infected cases and crude oil prices. In the top left corner, a red area is prominent in an edge-cutting shape pointing left and downward small arrows in a frequency region 0–4 and 4–8 during the 2nd and 3rd week of the observation. This coherence inferred a negative (out-phase) link between COVID-19 and crude oil prices and is characterized by anti-cyclical effect during this specific time–frequency realm. Another small oval shape in red-colored can be located at the top of the middle part in the cycle period 0–4 during the 12th week of the observation period. The direction of arrows from left and upward inside the oval shape implies anti-phase coherence directing from crude oil prices to COVID-19. This coherence infers a negative link between COVID-19 and crude oil prices and is characterized by an anti-cyclical effect during this specific time–frequency realm. The dark red color inside coincides with the correlation value of more than 0.90, and it reflects a robust COVID-19 impact on crude oil prices.

Figure 5c depicts the wavelet transform coherence between CO_2 emissions and crude oil prices. Some circular dark red colored shapes can be found incoherent across the figure within the thick black lining. By observing Fig. 5c, a circular shape can be located in frequency region 8–16 during the 13–18th week of the observation period.

The direction of arrows from left and upward inside the circular shape implies anti-phase coherence directing from crude oil prices to CO_2 emissions. This coherence infers a negative link between CO_2 emissions and crude oil prices and is also characterized by anti-cyclical effects during this specific time–frequency realm. Few but small red-colored areas with the black lining are apparent at frequency realm 4–8 during the 3rd, 4th, 12th, and 20th weeks of observation while the other edge-cutting island shape lies on the top left corner at the frequency spectrum 0–4 and 4–8 during the 2nd and 3rd week of the observation. The direction of arrows from left and upward inside the island's shape implies anti-phase coherence directing from crude oil price to CO_2 emissions. This coherence infers a negative link between CO_2 emissions and crude oil prices and also characterized by an anti-cyclical effect during this specific time–frequency realm. The dark red color of shapes is identical with the coherence value of almost equal or more than 0.90, and it reflects a robust COVID-19 effect on CO_2 emissions.

Figure 6a displays the results of partial wavelet coherence (PWC) relating to COVID-19, CO_2 emissions, and crude oil prices. In simple words, SPC correlation is a measurement tool for PWC between the COVID-19 and CO_2 emissions after eliminating the effects of crude oil prices. Several dark red colored oval and island shapes can be found incoherent across the figure within the thick black lining in a frequency region 0–4, 4–8 for short-term and 16–32 for long-term periods, respectively, which indicate coherence strength for a given period. Coherence for short-term period is witnessed during the 2nd and 6–7th weeks, whereas long term between the 8th and 11th weeks of the observation. The dark red color of shapes is identical, with the ranging of coherence value on the right side multi-colored bar from 0.90 to 1, reflecting strong coherence. From Fig. 5a, If we link this finding with the outcome of WTC for COVID-19 and CO_2 emissions, both results are seen to be identical. It is evident that the

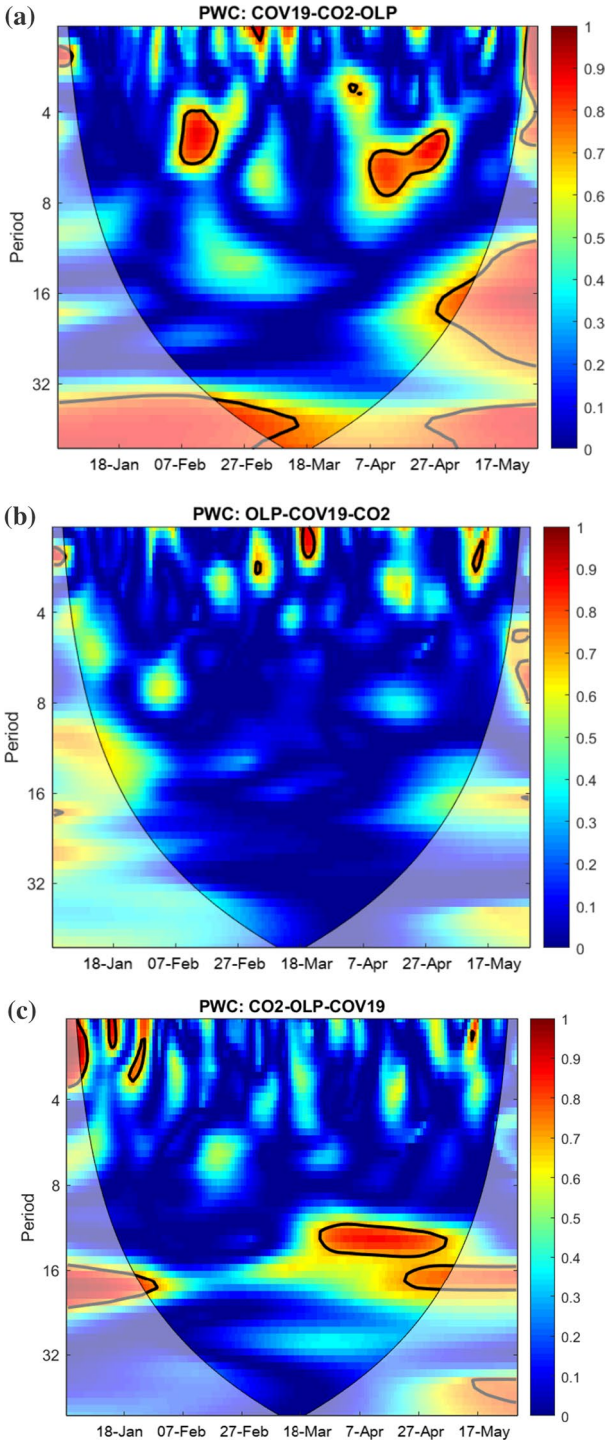

Fig. 6 Partial wavelet coherence of COVID-19, CO_2 emissions, and crude oil prices

prices of crude oil do not substantially impact the association between COVID-19 and CO_2 emissions, and WTC findings demonstrate the actual coherence between COVID-19 and CO_2 emissions.

Figure 6b displays the results of partial wavelet coherence (PWC) relating to the crude oil prices, COVID-19, and CO_2 emissions. More precisely, after eliminating the effects of CO_2 emissions, there tends to be a minimal coherence between crude oil prices and COVID-19, as apparent within the figure from the vast blue area. Considering the results of Fig. 5b, there exists an anti-phase (negative) link between COVID-19 and crude oil prices. It marked that the findings from PWC and WTC direct a substantial effect of CO_2 emissions on the association amid the crude oil prices and COVID-19.

Figure 6c displays the results of partial wavelet coherence (PWC) relating to the CO_2 emissions, crude oil prices, and COVID-19. More precisely, it shows the PWC between pair of CO_2 emissions and crude oil prices after canceling out the common properties of COVID-19. By observing Fig. 6c, the only noticeable difference is a small additional contour located at the right side in the last week at the frequency realm 4–8, which is missing in the case of WTC.

As earlier indicated, multiple wavelet coherence (MWC) mirrors the extent of co-movements of two-time series on a third one. Figure 7a equates to the MWC between COVID-19, CO_2 emissions, and crude oil prices. It portrays the outcome of MWC, relating COVID-19 as a predicted variable, whereas CO_2 emissions and crude oil prices as the predictor variables. The linear integration of these two CO_2 emissions and crude oil prices as predictor variables outlines the variations in COVID-19. Several dark red colored small and large circles with black outlines are apparent in all frequency bands 0–4, 4–8, 8–16, and 16–32 during the entire period from 2nd and 3rd, 6–7th, 8–12th, 15–17th, and 20th week of the observation, respectively. These small and large red-colored contours depict the combined intensity of CO_2 emissions and crude oil prices in predicting COVID-19.

Figure 7b displays the MWC upshot, relating crude oil price as a dependent variable while COVID-19 and CO_2 emissions as independent variables. Several large and small-shaped portrays in red-color can be ascertained in all frequency cycles 0–4, 4–8, 8–16, and 16–32 during the entire period from 1st, 3rd, 4th, 8th, 10th, 12–17th, and 20th week of the observation period. These shapes show the association strength with the crude oil prices and also depict the linear combination of COVID-19 and CO_2 emissions in that particular time–frequency domain.

Figure 7c corresponds to the MWC between CO_2 emissions, COVID-19, and crude oil prices. It portrays the result of MWC, relating CO_2 emissions as a dependent variable, whereas COVID-19 and crude oil prices as the independent variables. Several small and sizeable reddish circular and oval contours can be marked strewn across the figure within the thick black lining in all frequency bands 0–4, 4–8, 8–16, and onward during the 1st, 5th, 7th, 9–12th, 16–17th, and 19th weeks of the observation. These reddish contours depict combination intensity for crude oil prices and COVID-19 in forecasting CO_2 emissions. The shapes are more in red color, indicating the higher deviation that can be asserted in CO_2 emissions by the combined effect of crude oil prices and COVID-19.

4 Conclusion

This study explores the co-movement between COVID-19, CO_2 emissions, and crude oil prices by using the wavelet transform method. This paper strives to probe the causality of time–frequency within COVID-19, CO_2 emissions, and crude oil prices using a

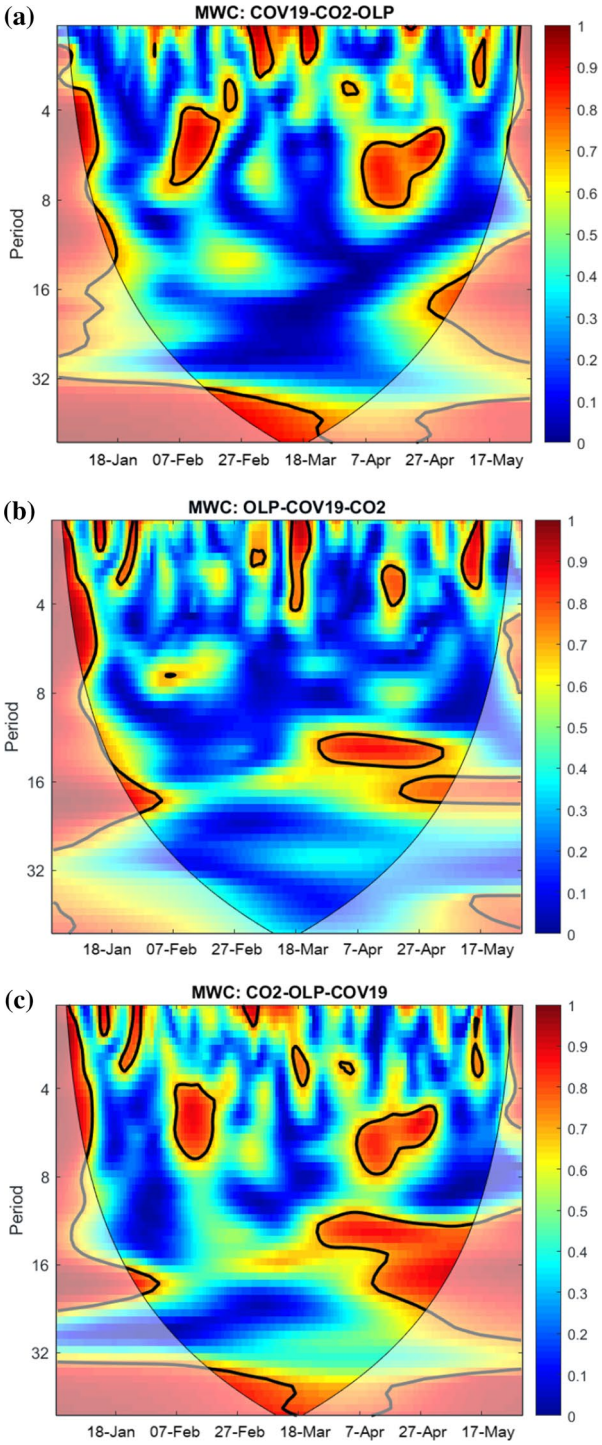

Fig. 7 Multiple wavelet coherence of COVID-19, CO_2 emissions, and crude oil prices

wavelet-based power spectrum, including continuous wavelet, wavelet coherence transform, partial, and multiple wavelet coherence. This method breaks down the time series into various time–frequencies and introduces the impacts relative to definite frequencies concentrating on all frequencies. The wavelet-based power spectrum approach allows one to examine dynamic lead–lag linkages in the time–frequency domain and to address some of the pragmatic complexities in the duration of short sampling and other schematic aspects like stationarity and nonlinearity. The paper uses daily data from December 31, 2019 to May 31, 2020.

This is the pioneer study on the environmental and economic effects of COVID-19. Hence, our findings provide several imperative fragments of evidence. First, the results of the continuous wavelet transform determine the significant and high energy patterns in small and medium periods but missing in a long period for COVID-19, CO_2 emissions, and crude oil prices. Second, in the short term, the results of wavelet transform coherence (WTC) witnessed the anti-phase (negative) link between COVID-19 and CO_2 emissions. In the long run, in-phase coherence is observed between COVID-19 and CO_2 emissions and finds CO_2 emissions is leading, and COVID-19 is lagging. Conversely, the other two combinations COVID-19 and crude oil prices; and CO_2 emissions and crude oil prices, WTC failed to find the existence of similar patterns of variance. For robustness, partial and multiple wavelet coherence (MWC) is applied and shows almost identical results. From the results, we conclude that, first, COVID-19 is expected to have a negative impact on economic stability in the long term. Second, the results indicate that COVID-19 impacts crude oil prices, which can be described by less oil demand due to curtailment in mobility and aviation. Third, COVID-19 is the most contributor to the reduction in CO_2 emissions during the pandemic period.

The findings of this study offer practical and policy implications. COVID-19 is a worldwide contagion and a significant menace to human health that hinders economic and social development. Conversely, it is a blessing and opportunity, where environmental pollution is minimized, and nature is regaining itself and reinstates. From this temporary assenting effect on climate, the findings portray the clear picture for environmentalists, governments, and individuals in what way to reduce emissions on a long-term basis. These findings are also essential for oil exploration and transport syndicates as well as investors with stock allocations that are inclined to the price of oil and commodity derivatives.

Authors contributions YH conceptualized the main idea, devised the methodology, administered the overall project, and wrote the original draft. EX supervised the overall research and validated the final results. ZF managed the resources and software. SHH executed the final review and editing of the manuscript.

Funding No funding source has been utilized for conducting this empirical research.

Availability of data and materials The datasets analyzed during the current study are available in the [Open Science Framework] repository, [https://osf.io/m4u6d/quickfiles].

Compliance with ethical standards

Conflict of interest The authors hereby declare that they have no competing interests with any person or organization.

References

Aloui, C., Hkiri, B., Hammoudeh, S., & Shahbaz, M. (2018). A multiple and partial wavelet analysis of the oil price, inflation, exchange rate, and economic growth nexus in Saudi Arabia. *Emerging Markets Finance and Trade, 54*(4), 935–956. https://doi.org/10.1080/1540496X.2017.1423469.

Anjum, N. (2020). Good in the worst: COVID-19 restrictions and ease in global air pollution. *Preprints*. https://doi.org/10.20944/preprints202004.0069.v1.

Aydın, S., Nakiyingi, B. A., Esmen, C., Güneysu, S., & Ejjada, M. (2020). Environmental impact of coronavirus (COVID-19) from Turkish perceptive. *Environment, Development and Sustainability*. https://doi.org/10.1007/s10668-020-00933-5.

BBC (2020). Coronavirus lockdown sees air pollution plummet across UK—BBC News. https://www.bbc.com/news/uk-england-52202974. Accessed 30 Jun 2020.

Benhmad, F. (2012). Modeling nonlinear Granger causality between the oil price and US dollar: A wavelet based approach. *Economic Modelling, 29*(4), 1505–1514. https://doi.org/10.1016/j.econmod.2012.01.003.

Carbon Brief (2020). Analysis: Coronavirus set to cause largest ever annual fall in CO2 emissions | Carbon Brief. https://www.carbonbrief.org/analysis-coronavirus-set-to-cause-largest-ever-annual-fall-in-co2-emissions?utm_source=Web&utm_medium=contentbox&utm_campaign=Covid-box. Accessed 30 Jun 2020.

Chan, J. F. W., Yuan, S., Kok, K. H., To, K. K. W., Chu, H., Yang, J., et al. (2020). A familial cluster of pneumonia associated with the 2019 novel coronavirus indicating person-to-person transmission: A study of a family cluster. *The Lancet, 395*(10223), 514–523. https://doi.org/10.1016/S0140-6736(20)30154-9.

Chen, N., Zhou, M., Dong, X., Qu, J., Gong, F., Han, Y., et al. (2020). Epidemiological and clinical characteristics of 99 cases of 2019 novel coronavirus pneumonia in Wuhan, China: A descriptive study. *The Lancet, 395*(10223), 507–513. https://doi.org/10.1016/S0140-6736(20)30211-7.

CNN (2020). Metro Manila air quality improves during quarantine. https://www.cnnphilippines.com/news/2020/3/25/metro-manila-improves-air-quality-amid-quarantine.html. Accessed 30 Jun 2020

Cucinotta, D., & Vanelli, M. (2020). WHO declares COVID-19 a pandemic. *Acta Biomedica*. https://doi.org/10.23750/abm.v91i1.9397.

Di Gennaro, F., Pizzol, D., Marotta, C., Antunes, M., Racalbuto, V., Veronese, N., et al. (2020). Coronavirus diseases (COVID-19) current status and future perspectives: A narrative review. *International Journal of Environmental Research and Public Health, 17*(8), 2690. https://doi.org/10.3390/ijerph17082690.

Dong, E., Du, H., & Gardner, L. (2020). An interactive web-based dashboard to track COVID-19 in real time. *The Lancet Infectious Diseases*. https://doi.org/10.1016/S1473-3099(20)30120-1.

Dutheil, F., Baker, J. S., & Navel, V. (2020). COVID-19 as a factor influencing air pollution? *Environmental Pollution*. https://doi.org/10.1016/j.envpol.2020.114466.

ESA. (2020). ESA—Air pollution remains low as Europeans stay at home. https://www.esa.int/Applications/Observing_the_Earth/Copernicus/Sentinel-5P/Air_pollution_remains_low_as_Europeans_stay_at_home. Accessed 30 June 2020

Gautam, S., & Hens, L. (2020a). SARS-CoV-2 pandemic in India: what might we expect? *Environment, Development and Sustainability*. https://doi.org/10.1007/s10668-020-00739-5.

Gautam, S., & Hens, L. (2020b). COVID-19: impact by and on the environment health and economy. *Environment, Development and Sustainability*. https://doi.org/10.1007/s10668-020-00818-7.

Gençay, R., Selçuk, F., & Whitcher, B. J. (2001). *An introduction to wavelets and other filtering methods in finance and economics*. Amsterdam: Elsevier.

Goodell, J. W., & Goutte, S. (2020). Co-movement of COVID-19 and Bitcoin: Evidence from wavelet coherence analysis. *Finance Research Letters*. https://doi.org/10.1016/j.frl.2020.101625.

Grinsted, A., Moore, J. C., & Jevrejeva, S. (2004). Application of the cross wavelet transform and wavelet coherence to geophysical time series. *Nonlinear Processes in Geophysics, 11*(5/6), 561–566. https://doi.org/10.5194/npg-11-561-2004.

Hkiri, B., Hammoudeh, S., Aloui, C., & Shahbaz, M. (2018). The interconnections between U.S. financial CDS spreads and control variables: New evidence using partial and multivariate wavelet coherences. *International Review of Economics and Finance, 57*, 237–257. https://doi.org/10.1016/j.iref.2018.01.011.

https://www.ecdc.europa.eu/en/covid-19-pandemic. (n.d.). COVID-19 pandemic. https://www.ecdc.europa.eu/en/covid-19-pandemic. Accessed 19 Jun 2020.

https://www.esrl.noaa.gov/gmd/obop/mlo/. (n.d.). ESRL Global Monitoring Division—Mauna Loa Observatory. https://www.esrl.noaa.gov/gmd/obop/mlo/. Accessed 19 Jun 2020.

Huang, C., Wang, Y., Li, X., Ren, L., Zhao, J., Hu, Y., et al. (2020). Clinical features of patients infected with 2019 novel coronavirus in Wuhan, China. *The Lancet, 395*(10223), 497–506. https://doi.org/10.1016/S0140-6736(20)30183-5.

IEA. (2020). Global energy and CO2 emissions in 2020—Global Energy Review 2020—Analysis —IEA. https://www.iea.org/reports/global-energy-review-2020/global-energy-and-co2-emissions-in-2020. Accessed 12 June 2020

Lai, C. C., Shih, T. P., Ko, W. C., Tang, H. J., & Hsueh, P. R. (2020). Severe acute respiratory syndrome coronavirus 2 (SARS-CoV-2) and coronavirus disease-2019 (COVID-19): The epidemic and the challenges. *International Journal of Antimicrobial Agents*. https://doi.org/10.1016/j.ijantimicag.2020.105924.

Le Quéré, C., Jackson, R. B., Jones, M. W., Smith, A. J. P., Abernethy, S., Andrew, R. M., et al. (2020). Temporary reduction in daily global CO2 emissions during the COVID-19 forced confinement. *Nature Climate Change*. https://doi.org/10.1038/s41558-020-0797-x.

Lu, H., Stratton, C. W., & Tang, Y. W. (2020). Outbreak of pneumonia of unknown etiology in Wuhan China: The mystery and the miracle. *Journal of Medical Virology*. https://doi.org/10.1002/jmv.25678.

Mate, A., Killian, J., Wilder, B., Charpignon, M., Awasthi, A., Tambe, M., et al. (2020). Evaluating COVID-19 lockdown policies for India: A preliminary modeling assessment for individual states. *SSRN Electronic Journal*. https://doi.org/10.2139/ssrn.3575207.

Mihanović, H., Orlić, M., & Pasarić, Z. (2009). Diurnal thermocline oscillations driven by tidal flow around an island in the Middle Adriatic. *Journal of Marine Systems, 78*(SUPPL. 1), S157–S168. https://doi.org/10.1016/j.jmarsys.2009.01.021.

Mitra, A., Ray Chadhuri, T., Mitra, A., Pramanick, P., & Zaman, S. (2020). Impact of COVID-19 related shutdown on atmospheric carbon dioxide level in the city of Kolkata. *Parana Journal of Science and Education, 6*(3), 84–92.

NASA. (2020). Data shows 30 percent drop in air pollution over northeast U.S. | NASA. https://www.nasa.gov/feature/goddard/2020/drop-in-air-pollution-over-northeast. Accessed 30 Jun 2020.

NASA Earth Observatory. (2020a). Airborne nitrogen dioxide plummets over China. https://earthobservatory.nasa.gov/images/146362/airborne-nitrogen-dioxide-plummets-over-china. Accessed 30 Jun 2020.

NASA Earth Observatory. (2020b). Airborne particle levels plummet in Northern India. https://earthobservatory.nasa.gov/images/146596/airborne-particle-levels-plummet-in-northern-india. Accessed 30 Jun 2020.

Ng, E. K. W., & Chan, J. C. L. (2012). Geophysical applications of partial wavelet coherence and multiple wavelet coherence. *Journal of Atmospheric and Oceanic Technology, 29*(12), 1845–1853. https://doi.org/10.1175/JTECH-D-12-00056.1.

OAG. (2020). Coronavirus and the impact on airline schedules. https://www.oag.com/coronavirus-airline-schedules-data. Accessed 12 Jun 2020.

Percival, D. B., & Walden, A. T. (2000). *Wavelet methods for time series analysis*. Cambridge: Cambridge University Press.

Ramsey, J. B. (2002). Wavelets in economics and finance: Past and future. *Studies in Nonlinear Dynamics and Econometrics*. https://doi.org/10.2202/1558-3708.1090.

Sohrabi, C., Alsafi, Z., O'Neill, N., Khan, M., Kerwan, A., Al-Jabir, A., et al. (2020). Corrigendum to "World Health Organization declares Global Emergency: A review of the 2019 Novel Coronavirus (COVID-19)" [Int. J. Surg. 76 (2020) 71–76]. *International Journal of Surgery, 77*, 217. https://doi.org/10.1016/j.ijsu.2020.03.036.

The Conversation. (n.d.). Coronavirus: Lockdown's effect on air pollution provides rare glimpse of low-carbon future. https://theconversation.com/coronavirus-lockdowns-effect-on-air-pollution-provides-rare-glimpse-of-low-carbon-future-134685. Accessed 30 Jun 2020.

Torrence, C., & Compo, G. P. (1998). A practical guide to wavelet analysis. *Bulletin of the American Meteorological Society, 79*(1), 61–78. https://doi.org/10.1175/1520-0477(1998)079<0061:APGTWA>2.0.CO;2.

Torrence, C., & Webster, P. J. (1999). Interdecadal changes in the ENSO–Monsoon system. *Journal of Climate, 12*(8), 2679–2690. https://doi.org/10.1175/1520-0442(1999)012<2679:icitem>2.0.co;2.

Tosepu, R., Gunawan, J., Effendy, D. S., Ahmad, L. O. A. I., Lestari, H., Bahar, H., et al. (2020). Correlation between weather and Covid-19 pandemic in Jakarta Indonesia. *Science of the Total Environment, 725*, 138436. https://doi.org/10.1016/j.scitotenv.2020.138436.

Urrutia-Pereira, M., Mello-da-Silva, C. A., & Solé, D. (2020). COVID-19 and air pollution: A dangerous association? *Allergologia et Immunopathologia, 48*(5), 496–499. https://doi.org/10.1016/j.aller.2020.05.004.

Vacha, L., & Barunik, J. (2012). Co-movement of energy commodities revisited: Evidence from wavelet coherence analysis. *Energy Economics, 34*(1), 241–247. https://doi.org/10.1016/j.eneco.2011.10.007.

Wang, P., Chen, K., Zhu, S., Wang, P., & Zhang, H. (2020). Severe air pollution events not avoided by reduced anthropogenic activities during COVID-19 outbreak. *Resources, Conservation and Recycling, 158*, 104814. https://doi.org/10.1016/j.resconrec.2020.104814.

WHO. (2020a). Transmission of SARS-CoV-2: Implications for infection prevention precautions.

WHO. (2020b). WHO | World Health Organization. https://www.who.int/. Accessed 9 Jun 2020.

WHO. (2020c). Q&A on coronaviruses (COVID-19). https://www.who.int/emergencies/diseases/novel-coronavirus-2019/question-and-answers-hub/q-a-detail/q-a-coronaviruses. Accessed 25 Sep 2020.

Wilder-Smith, A., & Freedman, D. O. (2020). Isolation, quarantine, social distancing and community containment: Pivotal role for old-style public health measures in the novel coronavirus (2019-nCoV) outbreak. *Journal of Travel Medicine*. https://doi.org/10.1093/jtm/taaa020.

Xu, Z., Shi, L., Wang, Y., Zhang, J., Huang, L., Zhang, C., et al. (2020). Pathological findings of COVID-19 associated with acute respiratory distress syndrome. *The Lancet Respiratory Medicine, 8*(4), 420–422. https://doi.org/10.1016/S2213-2600(20)30076-X.

Zhou, F., Yu, T., Du, R., Fan, G., Liu, Y., Liu, Z., et al. (2020). Clinical course and risk factors for mortality of adult inpatients with COVID-19 in Wuhan, China: A retrospective cohort study. *The Lancet, 395*(10229), 1054–1062. https://doi.org/10.1016/S0140-6736(20)30566-3.

Affiliations

Yasir Habib[1] · Enjun Xia[1] · Zeeshan Fareed[2] · Shujahat Haider Hashmi[3]

✉ Yasir Habib
yasirhabib.ch@outlook.com

Enjun Xia
enjunxia@bit.edu.cn

Zeeshan Fareed
zeeshanfareed@hotmail.com

Shujahat Haider Hashmi
shujahat_hashmi@hotmail.com

[1] School of Management and Economics, Beijing Institute of Technology, Beijing 100081, China

[2] School of Business, Huzhou University, Huzhou, Zhejiang, China

[3] School of Economics, Huazhong University of Science and Technology, Wuhan, China